Tropical Natural History 24 (2024): 48-59

# Description of the Larva of *Argiocnemis rubescens rubeola* Selys, 1877 (Odonata, Coenagrionidae, Agriocnemidinae) from Thailand with Systematic Notes on the Subfamily Agriocnemidinae

**TOSAPHOL SAETUNG KEETAPITHCHAYAKUL[1], RYO FUTAHASHI [2], PATCHARA DANAISAWADI[3], KAEWPAWIKA JITTHAMMA IGNATIUS[4] AND KORAON WONGKAMHAENG[3]***

*[1] The Center for Entomology & Parasitology Research, College of Medicine and Pharmacy, Duy Tan University, 120 Hoang Minh Thao, Lien Chieu, Da Nang, VIETNAM*
*[2] Bioproduction Research Institute, National Institute of Advanced Industrial Science and Technology (AIST), Tsukuba 305-8566, JAPAN*
*[3] Department of Zoology, Faculty of Science, Kasetsart University, Bangkok, 10900, THAILAND*
*[4] Forest and Plant Conservation Research Office, Department of National Parks, Wildlife and Plant Conservation, Bangkok 10900, THAILAND*
*Corresponding author. koraon wongkamhaeng (Koraon@gmail.com)
Received: 9 October 2023; Accepted: 20 February 2024

**ABSTRACT. –** The final stadium larvae of *Argiocnemis rubescens rubeola* are described in the present study. The adult–larva association along with the taxonomic remarks on the subfamily Agriocneminae, is established by employing the cytochrome oxidase subunit I gene (*COI*). The larva is characterized by the ovate shape of the caudal lamella, the lack of a band on the caudal lamella, a rounded postocular lobe outline, three pairs of premental setae, and four palpal setae. Taxonomic notes suggest the *COI* data consistently aligns with both larval and adult characteristics, offering a comprehensive perspective.

**KEYWORDS: *Argiocnemis*, Agriocnemidinae, Coenagrionidae, *COI*, Thailand**

## INTRODUCTION

*Argiocnemis* Selys, 1877 is a small genus belonging to the subfamily Agriocnemidinae (Dijkstra et al., 2014). Three species have been recorded around the world, *A. ensifera* Lieftinck, 1932, *A. solitaria* (Selys, 1872), and *A. rubescens* Selys, 1877 listed in Paulson et al. (2023). While *A. ensifera* and *A. solitaria* are endemic species from the Papuan and East African regions, respectively (Clausnitzer and Martens, 2004; Kalkman and Orr, 2013), *A. rubescens* is widely distributed from South Asia eastward to the Australasia region. The taxonomic status of *A. rubescens* is uncertain and poorly studied. Previously, many odonatologists treated *A. rubescens* from each region as a subspecies (*A. r. rubescens*: Australia, Sumatra, Java, Sumba; *A. r. intermedia*: Philippine Islands; *A. r. lunulata*: Philippine Islands, Java, Sulawesi; *A. r. nigricans*: New Guinea; *A. r. obscura*: Assam; *A. r. rubeola*: Indochina, Luzon, Sulawesi, Sumatra,) (Lieftinck, 1954; Asahina, 1993; Steinmann, 1997; Dow, 2011; Dijkstra et al., 2014).

In the case of *Argiocnemis* larva, illustrations of the head and caudal lamella of *Argiocnemis rubescens* from Australia (*A. r. rubescens*) were proposed by Theischinger and Hawking (2006) and Theischinger and Endersby (2009), although the larva stage of *A. ensifera* and *A. solitaria* have not been described. Recently, Saetung and Boonsoong (2019) proposed a diagnosis of the larval characteristics of the genus *Argiocnemis* partly based on details provided by Morse et al. (1994). Unfortunately, the larval figures of *A. rubescens* in Morse et al. (1994) are likely to be mistaken because they should belong to *Ceriagrion aeruginosum* (Brauer, 1869) based on Needham (1930). Thus, the larval description of the *A. rubescens* requires clarification.

The taxonomic status of the subfamily Agriocneminae remains uncertain, and efforts to understand the relationships within the subfamily have been explored in studies by Dow (2011), with a particular focus on genital ligula. Saetung and Boonsoong (2019) further divided the Asian *Agriocnemis* into two groups, distinguished by larval and male genital ligula characteristics, and specifically categorized as the *minima*- and *femina*- groups.

The present study provides a description of the final stadium larva of *Argiocnemis rubescens rubeola*. The adult–larva association of *A. r. rubeola* and the taxonomic notes of the subfamily Agriocneminae are accomplished through the utilization of the cytochrome oxidase subunit I gene (*COI*).

## MATERIALS AND METHODS

### Molecular study

The twelve specimens of subfamily Agriocnemidinae and a single *Ischnura rufostigma* specimen were used in the molecular study (Table 1). Total DNA was extracted from legs using a genomic DNA purification kit (DNeasy Blood and Tissue Kit [Qiagen, Germany]),

**TABLE 1.** List of sequenced specimens.

| Species | Stage/Sex | Collection locality | Code | Genbank /BOLD accession number |
|---|---|---|---|---|
| *Argiocnemis rubescens rubeola* | adult/ male | Krabi/ Thailand | ArgRub-AM | MT942601 |
| *Argiocnemis rubescens rubeola* | adult/ female | Ratchaburi / Thailand | ArgRub-AF | MT942602 |
| *Argiocnemis rubescens rubeola* | larva/female | Kanchanaburi / Thailand | ArgRub-LM | MT942603 |
| *Argiocnemis rubescens rubeola* | larva/ male | Nakhon Nayok / Thailand | ArgRub-LF | MT942604 |
| *Agriocnemis nana* | adult/ male | Prachinburi / Thailand | AgrNan-AM | private |
| *Agriocnemis nana* | adult/ female | Prachinburi / Thailand | AgrNan-AF | private |
| *Agriocnemis nana* | larva/ male | Prachinburi / Thailand | AgrNan-LM | private |
| *Agriocnemis minima* | larva/ male | Prachinburi / Thailand | AgrMin-LM | private |
| *Agriocnemis pygmaea* | Adult / male | Okinawa / Japan | AgrPyg-A | private |
| *Agriocnemis femina* | Adult / female | Kochi / Japan | AgrFem-A | private |
| *Mortornagrion hirosei* | adult/female | Yamaguchi / Japan | Mor-Hir-A | private |
| *Mortornagrion selenion* | adult/female | Toyama / Japan | MorSel-A | private |
| *Ischnura rufostigma* | larva/male | Chaing Mai / Thailand | IscRuf-LM | private |

following the manufacturer's instructions. The *COI* fragment was amplified using the primers LCO1490 (5'–GGT CAA ATC ATA AAG ATA TTG G–3') and HCO2198 (5'–TAA ACT TCA GGG TGA CCA AAA AAT CA–3') (Folmer et al., 1994). 25 microliters of the PCR reaction mix composed of 5 µl of ultrapure water, 5 µl of DNA template, 1.5 µl of each primer (10 µM), and 12 µl of master mix. The PCR reaction was conducted with an initial step of 94°C for 5 minutes followed by a total of 40 cycles at 94°C for 30 seconds, 52°C for 20 seconds, 72°C for 60 seconds, and 72°C for 5 minutes. Purification and bi–directional Sanger sequencing was performed by Macrogen, Inc. (South Korea).

The seventeen sequences from GenBank and this study (Table 2) were edited and assembled in BioEdit v7.2.0 (Hall, 1999). Multiple sequence alignments were performed using ClustalX version 2.1. Pairwise genetic distances were calculated using Kimura's two-parameter model (K2P) in MEGA X (Kumar et al., 2018).

## Phylogenetic analyses and species delimitation

Phylogenetic trees were constructed using maximum likelihood (ML) and Bayesian inference (BI). Prior to the ML and BI analyses, the best-fit models of nucleotide substitution were identified separately with the three codon positions of *COI* sequences using MEGA X (Kumar et al., 2018). ML phylogenetic analysis was performed by applying the GTRGAMMA model at the default settings of raxmlHPC-PTHREADS-SSE3 on raxmlGUI 2.0. Nodal support values of ML were assessed with 1,000 bootstraps (Edler et al., 2020). BI analysis was performed using MrBayes 3.1.2 (Huelsenbeck and Ronquist, 2001). For each dataset, four independent Monte Carlo Markov Chain simulations were run with four chains for ten million generations where the temperature value was lowered to 0.15, the average standard deviation of split frequencies dropped to approximately 0.005, and the trees were sampled at every 1,000 generations. All sampled topologies beneath the asymptote (25%) were discarded as part of a burn-in procedure. The majority rule 50% posterior probability trees were obtained as consensus final topologies after burning 25% of the generations. Consensus trees were then displayed and rendered with FigTree v1.4.0 (Rambaut, 2012).

The molecular operational taxonomic units (MOTUs) delimited by the two species delimitation analyses were regarded as preliminary hypothesis: the distance-based ASAP (Assemble Species by Automatic Partitioning; Puillandre et al., 2020) and the tree-based

**TABLE 2.** List of sequence from GenBank.

| Species | Collection locality | BOLD/Genbank accession number | Reference |
|---|---|---|---|
| *Argiocnemis rubescens* | Thailand | MK506261 | Saetung and Boonsoong (2019) |
| *Argiocnemis rubescens rubeola* | Malaysia | KF369308 | Dijkstra et al. (2014) |
| *Argiocnemis rubescens rubescens* | Indonesia | KF369309 | Dijkstra et al. (2014) |
| *Agricnemis pygmaea* | Thailand | MK506258 | Saetung and Boonsoong (2019) |
| *Agricnemis pygmaea* | Thailand | KT957454 | Thipaksorn and Ruangsittichai (2010) |
| *Agricnemis pygmaea* | Pakistan | MAODO136-10 | - |
| *Agricnemis femina* | Thailand | MK506260 | Saetung and Boonsoong (2019) |
| *Agricnemis femina* | Thailand | KT957459 | Thipaksorn and Ruangsittichai (2010) |
| *Agricnemis minima* | Thailand | MK506259 | Saetung and Boonsoong (2019) |
| *Agricnemis minima* | Thailand | KT957461 | Thipaksorn et al. (2012) |
| *Agricnemis forcipata* | Gabon | KF369284 | Dijkstra et al. (2014) |
| *Agricnemis canuango* | Angola | KU565901 | Dijkstra et al. (2015) |
| *Agricnemis canuango* | Angola | KU565899 | Dijkstra et al. (2015) |
| *Agricnemis toto* | Angola | KU565902 | Dijkstra et al. (2015) |
| *Agricnemis toto* | Angola | KU565904 | Dijkstra et al. (2015) |
| *Mortanagrion martini* | Papua New Guinea | KF369453 | Dijkstra et al. (2014) |
| *Mortanagrion stygium* | Congo | KF369454 | Dijkstra et al. (2014) |

PTP (Poisson Tree Processes; Zhang et al., 2013) approaches. The ASAP was applied to *COI* alignment using the ASAP web-server available at https://bioinfo.mnhn.fr/abi/public/asap/asapweb.html, computing the genetic distances under simple p-distances with all other settings set to default. The PTP was conducted on the web service available at https://mptp.h-its.org, with the ML tree used as the Input for the PTP, the partition with the lowest score was selected, and all the other settings were set to their defaults. The adult–larva association was matched based on COI gene to ensure that the adult and larva are the same species based on MOTUs.

## Morphological study

*Argiocnemis* larvae were collected from forests and agricultural ponds in Thailand. A sweep net was used to capture adults around larval habitats. The examined specimens were preserved in absolute ethanol. Adult identification was performed at the species level based on male caudal appendages genital ligula and female prothorax (Fig.1) following Fraser (1934) and Dow (2011). Measurements (mm) and photographs were obtained using a NIKON SMZ800 and a Nikon D750 with a Nikon 105 f/2.8 macro lens and a Laowa 25 mm f/2.8 2.5–5x ultra macro lens. The photos were stacked

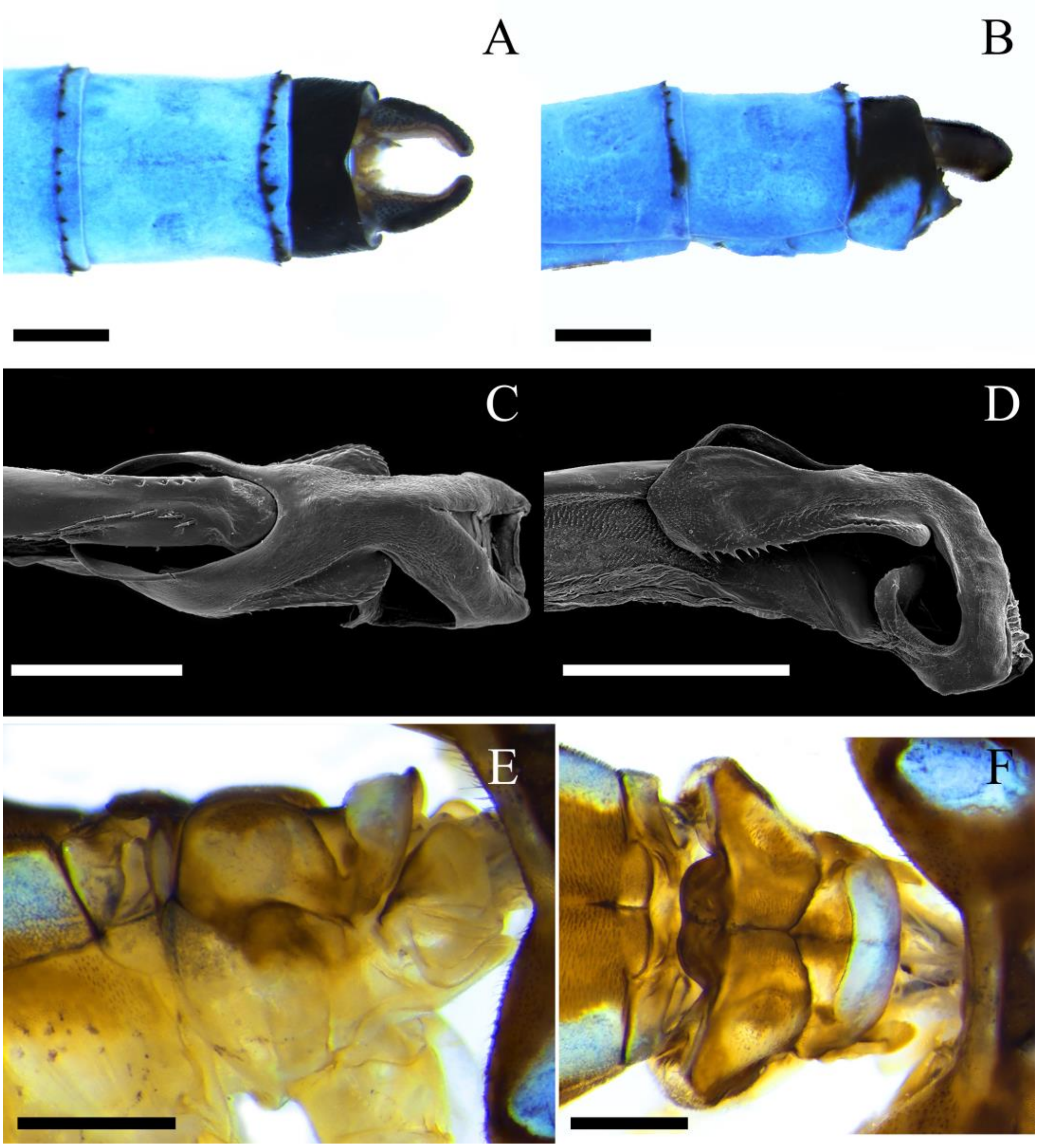

**FIGURE 1.** Diagnosis characters for identified adults of *Argiocnemis rubescens rubeola*: (A–D) male; (E–F) female; (A) caudal appendages, dorsal view; (B) caudal appendages, lateral view; (C) genital ligula, ventral view, SEM photo; (D) Genital ligula, lateral view, SEM photo; (E) prothorax, lateral view; (F) prothorax, dorsal view. Scale (B–C) = 0.2 mm; (A, B, E, F) = 0.25 mm.

using Helicon Focus software. All illustrations were made using the Procreate application on an iPad Pro 2020 based on a representative digital photograph. Final plates were prepared using Adobe Photoshop CC 2017. The genital ligula specimens were dehydrated with absolute ethanol, critical–point dried using carbon dioxide, placed on holders, and coated with gold for examination using an FEI Quanta 450 scanning electron microscope. The caudal gills and mandible terminology are in line with Tillyard (1917) and Watson (1956), whereas segments 1–10 were indicated as S1–S10, and antennomeres 1–7 were indicated as A1–A7. Voucher specimens were deposited at Keetapithchayakul's personal collection.

## RESULTS

### Molecular analysis

### Phylogenetic analyses and species delimitation

The maximum likelihood (ML) and Bayesian inference (BI) tree are summarized in Fig. 2, with posterior probabilities (PP) and bootstrap support values (BS) from the corresponding BI and ML analysis included. Although the 50% cut-off support value of the BI and ML tree (50% majority tree) were used to judge those of clade be forming polytomy, however, the low support (PP<0.85 and BS<75) indicates that the clade collapsed as polytomy with upper clade.

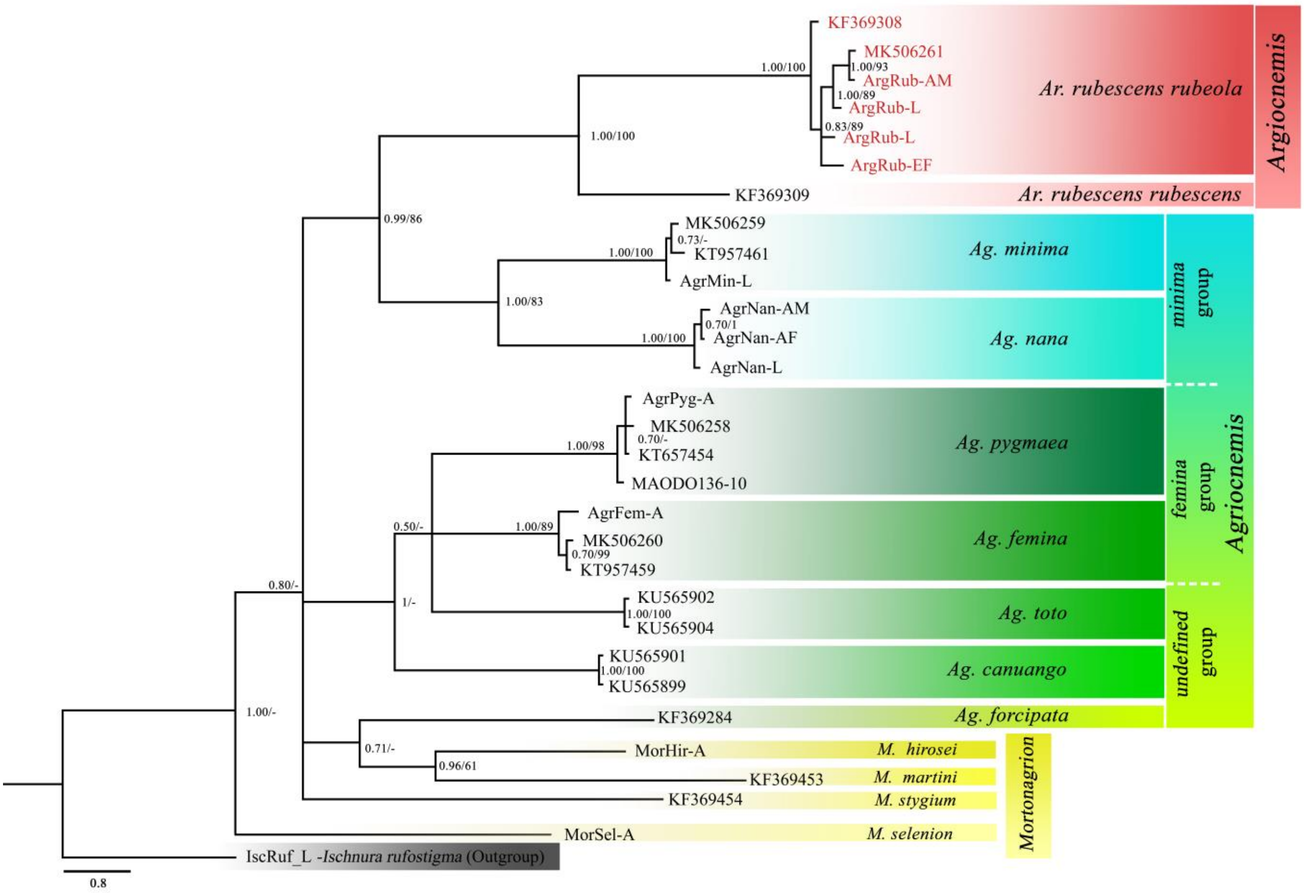

**FIGURE 2.** *COI* tree of subfamily Agriocnemidinae. Values of posterior probabilities and bootstraps support are indicated at nodes. Horizontal bars indicated results of species delimitation analyses using ASAP and PTP. Vertical bar indicated species within each genera of subfamily Agriocnemidinae.

The partial *COI* tree exhibited the lowest resolution on the upper node. The *Argiocnemis* clade demonstrated that the larva and adult *Argiocnemis rubescens rubeola* formed a monophyletic clade (PP=1.00, BS=100), while *Argiocnemis r. rubescens* also formed a sister group with *Argiocnemis r. rubeola* clade (P =1.00, BS=100). Interestingly, clades of *Agriocnemis* are a paraphyletic group. The clades of *Agriocnemis minima* and *Agriocnemis nana* performed a monophyletic clade as being sister clade with the genus *Argiocnemis* (PP = 0.99, BS=86). Another clade of *Agriocnemis* collapsed in a basal polytomy except *Agriocnemis forcipata* clade with high support (PP=0.8, BS=100). These *Agricnemis* clades consist of Afrotropical species (*Agriocnemis forcipata*, *Agriocnemis canuango*, and *Agriocnemis toto*) and Asian species (*Agriocnemis femina* and *Agricnemis pygmaea*). The genus *Mortonagrion* and *A. forcipata* performed as individual clades in which *M. hirosei* and *M. martini* were grouped (PP=0.96, BS=61).

The species delimitation indicated that the number of MOTUs was equal to those identified by morphospecies. The results of the distance-based approach (ASAP) recovered 13 MOTUs, respectively, while the tree-based approach also indicated 13 MOTUs (Fig. 2). Therefore, both species delimitation analyses suggested that species delimitation of partial *COI* gene supports the adult–larva association of *Argiocnemis rubescens rubeola*.

## Genetic distance

The uncorrected pairwise genetic distances among the thirteen species of the subfamily Agriocnemidinae are presented in Supplement Materials, Table S1. The intraspecific genetic distance ranged from 0.00% to 1.85%, whereas the interspecific genetic distance ranged from 11.40% to 25.29%. For *Argiocnemis rubescens rubeola*, genetic distance of the larvae differs in just 0.15–1.85% from the adults, while other samples of six *Agriocnemis* spp. differs in 0.00%–0.92% in the same species. However, *A. r. rubeola* also presents a high uncorrected pairwise genetic distance (12.94%–14.06%) with *A. r. rubescens*.

## Larval description of *Argiocnemis rubescens rubeola* (Selys, 1877)

The individuals examined were as follows: 2 exuviae (last stadium larvae from the collection site which were then reared in the laboratory) 1 male and 1 female, 26/XI/2020, Kang Som Meaw Pond (13°24’36.5”N, 99°16’33.3”E, altitude 209 m), Ratchaburi Province, Thailand, T.S. Keetapithchayakul leg.; 7 last stadium larvae including 1 male, 9/VI/2017, Khao Khitchakut National Park (12°50’19.3”N, 102°07’11.6”E, altitude 65 m) Chanthaburi Province, Thailand; K. Rattanachan leg.; 1 male and 1 female, 26/XI/2020, Kang Som Meaw Pond (13°24’36.5”N, 99°16’33.3”E, altitude 209 m), Ratchaburi Province, Thailand, T.S. Keetapithchayakul leg.; 1 male and 1 female, 10/XI/2018, Mae Kwa, (14°29’05.9”N, 99°00’31.7”E, altitude 207 m), Kanchanaburi Province, Thailand, K. Rattanachan leg., 1 male and 1 female, 4/IV/2021, Wang Ta Krai Pond, (14°19’25.8”N, 101°18’18.9”E, altitude 38 m), Nakhon Nayok Province, Thailand, T.S. Keetapithchayakul leg.; 1 male, 4/IV/2021, Inthanon Lady's Slipper Orchid Conservation Project, Doi Inthanon National Park (18°35’05.4”N, 98°30’45.0”E), Chiang Mai Province, Thailand, T.S. Keetapithchayakul leg.

## Description of the larva

***Body*:** Slender (Fig.3), pale yellowish-cream to yellowish-brown or greenish-yellow.

*Head*: Subpentagonal, the head width exceeds 1.13 times the head length, wider than the thorax and abdomen. Labrum distal half covered with sparse simple setae; anterior margin flattened ventrally with sparse simple setae. Clypeus with sparse small simple setae and small brown spots. Frons and vertex are glabrous with three prominent ocelli. Concave occiput mostly glabrous. Postocular lobes curvilinear in outline with several scattered spiniform setae. Compound eyes narrow and rounded protruding posterolateral side. Antennae (Fig. 4A) filiform, longer than 1.30 times the head length, 7-segmented with A3 the longest; relative length of antennomeres 0.88:0.78: 1.00 (0.50 mm): 0.72: 0.51: 0.36: 0.25; scape (A1) as wide as 1.38 and 3.72 times pedicel (A2) and A3 width, with scattered small and long simple setae; pedicel with scattered small and long simple setae; A3–A7 with small simple setae. Genae (Fig. 4B) glabrous, with row of 6–10 small stout spiniform setae. Labium (Fig. 4C) articulation of prementum and postmentum extended at the level of middle coxae of foreleg to anterior coxae of midleg; prementum with three pairs of premental setae, a row of 12–17 small spiniform setae along the distal half of lateral margins, laterodistal margin with 2–3 spiniform setae; ligula (Fig. 4D) prominent spoon-shaped, scattered small simple setae, one pair of small protuberances and 45–49 minute spiniform setae along margin; sub-quadrangular postmentum with simple setae on ventral side; labial palp (Fig. 4E) as long as 0.52 times the prementum length, with four palpal setae on each side, apical lobe ending with two lobes forming a truncate, denticulate lobe with five distinct teeth and one small tooth and end hook, a movable hook slender and pointed and 0.54× as long as the palp length. Maxilla (Fig. 4F, G) galeolacinia with six teeth, three ventral teeth of different sizes and robustness of which apical tooth largest, and the basal tooth is preceded by a row of four distinct setae, three dorsal teeth similar in length and robustness, incurved. Mandible (Fig. 5) with distinct teeth on each incisor lobe, without a molar crest, with 3–5 simple setae on the outer side; right mandible (Fig. 5A, B) with five incisors, single molar tooth, one addition tooth, left mandible (Fig. 5C, D) with five incisor teeth, two molar teeth (a = b); following mandibular formula: L 1+1’234 0 a b/ R 1+1’234 y a.

***Thorax*:** Middle lobe of prothorax with a small shallow groove in the middle; pronotum subtrapezoidal with scattered simple setae, lateral margins almost concave, posterolateral region protruding, pronotal disc smooth. Synthorax scattered simple setae. Wing pads parallel, anterior and posterior wing pads reaching almost abdominal S5. Legs almost flat and long; femora thin with a dark band on the posterior side and scattered simple setae, hind femora as long as 1.67 and 1.21-times the length of the fore and mid femora. Tibiae comb with scattered tridentate setae, a few simple setae. Tarsi with two rows of tridentate setae.

***Abdomen*:** Slender and cylindrical, narrowed caudally, abdominal terga with scattered simple setae, spiniform setae two longitudinal pale black stripes on midline; abdominal sterna with a pale network of tracheoles, with dark spots on posterolateral side; abdominal pleura with row of setae, abdominal pleura S1–S8 flattened, narrowed caudally, with simple setae and spiniform setae along the lateral margin and distinct spiniform setae on the posterolateral end, abdominal S10 three distinct concave, posterior margin with cluster of spiniform setae externally at the basal of cerci; Male gonapophyses (Fig. 6A, B); small, sharply pointed, weakly divergent in ventral view. Gonopore tiny, O-shape, embossed and fissure on middle to posterior. Male cerci prolate sub–spheroid shape, rounded tip. Female gonapophyses (Fig. 6C, D) with lateral valves slightly divergent, tips sharply pointed; lateral valves extending to posterior margin of S10, with a row of setae along ventral margin; central valves slender, apically rounded, and slightly shorter than

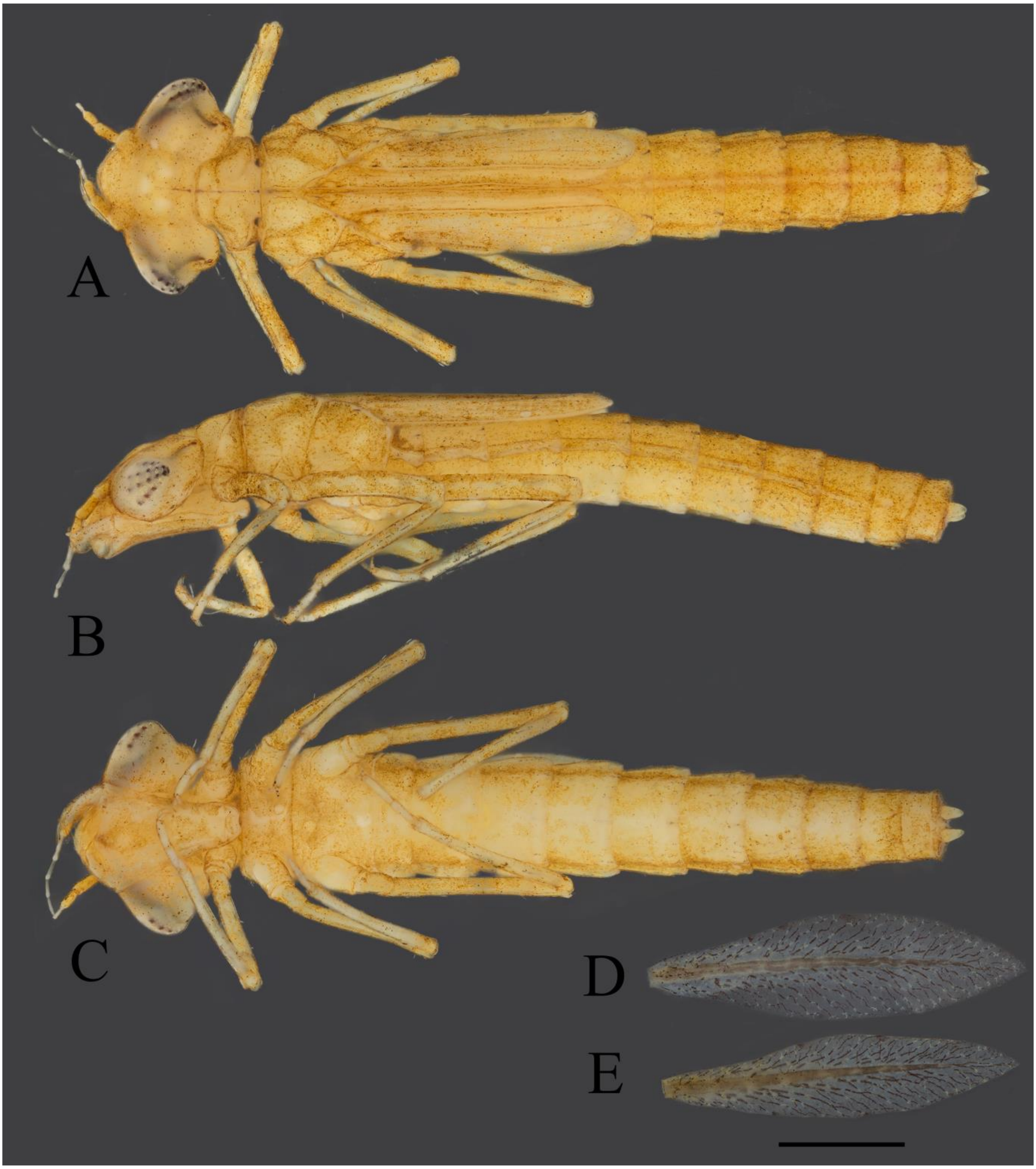

**FIGURE 3.** Larval habitus and caudal lamella detached of *Argiocnemis rubescens rubeola*: (A, B, C) larval habitus; (D, E) caudal lamella; (A) dorsal view; (B) lateral view; (C) ventral view. Scale = 1.5 mm.

lateral valves; female cerci with a small cone and blunted tip. Caudal lamellae (Fig. 6A, B) transparent, denodate with pointed tip and wider in the middle; median trachea, yellowish-cream, largest, distinct, reaching 5/6 of caudal lamellae, secondary branches, brown intermingled pale cream, irregularly branched, little undulate extended to distal margin, tertiary branches arise to margin side, with scattered small quaternary branches on last branches; median gill (Fig. 7A–C) with 18–24 spiniform setae on the dorsal margin and sparsely 8–12 spiniform setae on ventral margin, median trachea with 13–18 spiniform setae

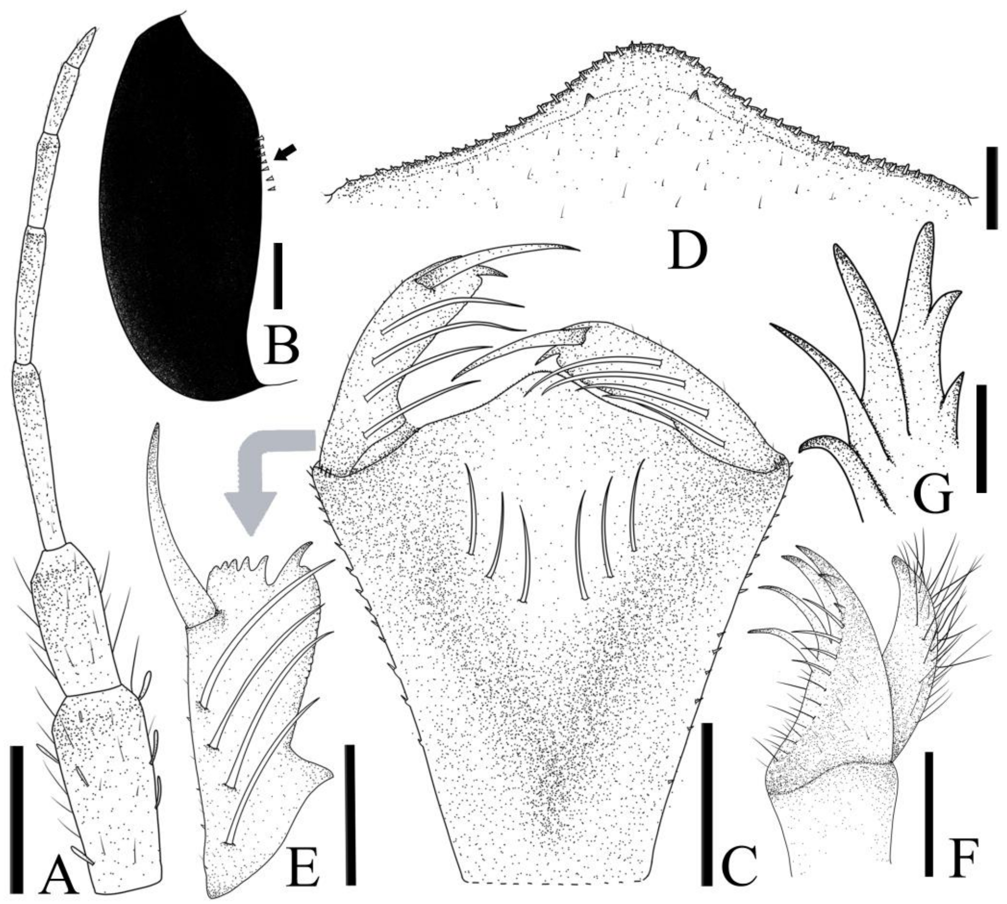

**FIGURE 4.** Antenna, genae, and mouth parts of *Argiocnemis rubescens rubeola* larva: (A) right antenna; (B) right genae, arrow = row of spiniform setae, (C) labium, dorsal view, (D) ligula, dorsal view; (E) left labial palp in dorsolateral view; (F) right maxilla, ventral view; (G) right lacinia teeth, internal view. Scale = (A) 1 mm, (B, E, F, G) 0.25mm, (C) 0.5 mm, (D) 0.1 mm.

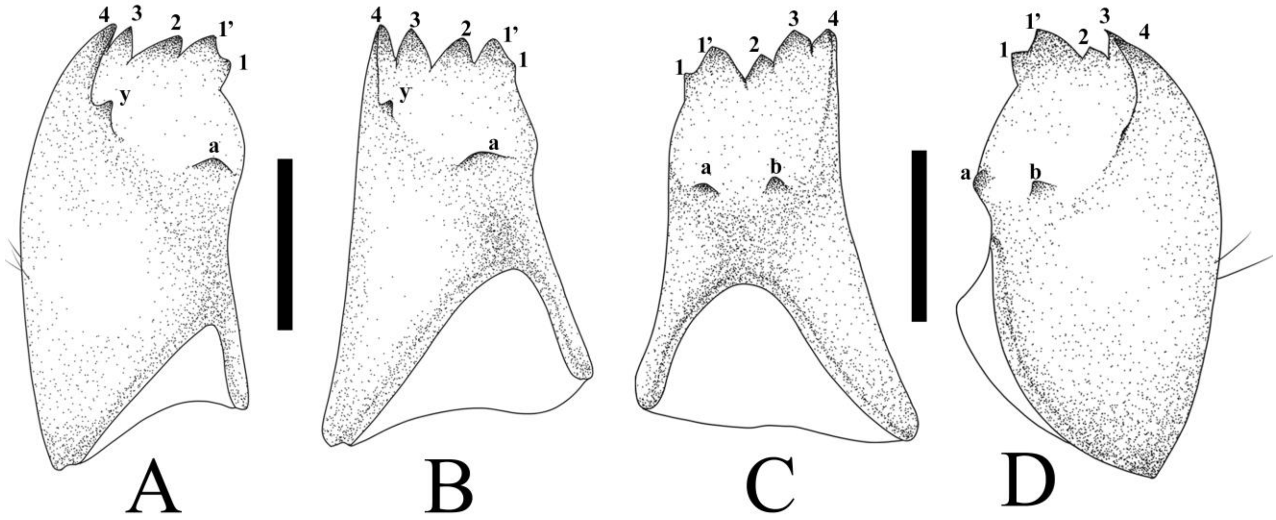

**FIGURE 5.** Mandible of *Argiocnemis rubescens rubeola* larva: (A) right mandible, ventrolateral view; (B) right mandible, internal view; (C) left mandible, internal view. (D) left mandible, ventrolateral view. Scale = 0.25 mm.

array on both sides; lateral gills (Fig. 7B) with 6–10 spiniform setae on ventral margin with 21–27 spiniform setae on dorsal margin and with 8–13 spiniform setae along lateral margins of median trachea.

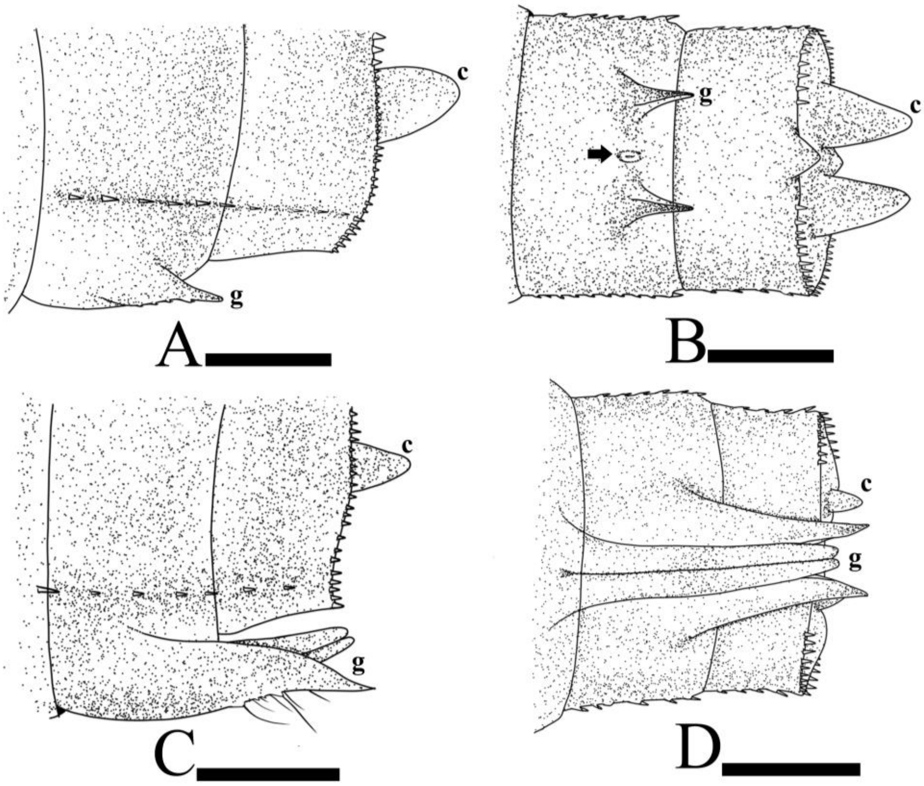

**FIGURE 6.** Abdominal S8–S10 of *Argiocnemis rubescens rubeola larva*: (A, B) male; (C, D) female; (A, C) lateral view; (B, D) ventral view. Scale = 0.25 mm (arrow= gonopore, c = cerci, g = gonapophyses).

***Measurements.—*** [in mm; n =10; (3 exuviae and 7 alcoholic specimens)] total length of body without caudal lamellae = 16.54–18.63; length of caudal lamellae = 4.52–5.43; width of head = 1.65–1.93; length of antenna = 7.89–8.93; width and length of prementum =1.09–1.17 and 1.75–1.92; length of labial palp = 0.92–0.98; length of movable hook = 0.48–0.52; length of inner and outer wing pads = 4.10–4.52 and 4.13–4.24; length of femora (fore: mid: hind) = 1.49–1.79: 2.07–2.11: 2.47–2.58; length of tibiae (fore: mid: hind) = 1.78–1.86: 1.97–2.06: 2.43–2.74; length of tarsi (fore: mid: hind) = 0.77–0.83: 0.92–0.97: 0.97–1.03.

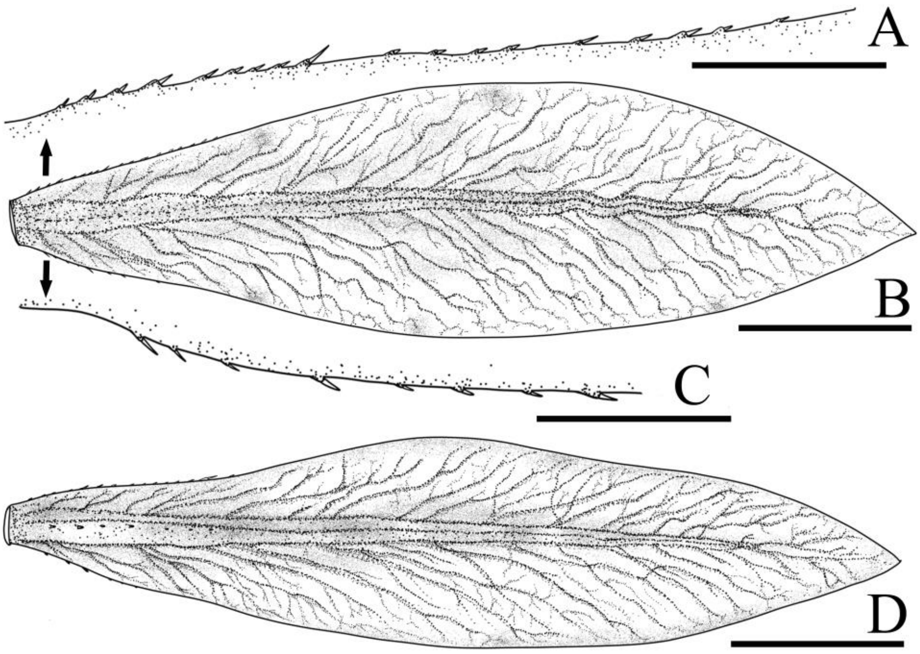

**FIGURE 7.** Caudal lamellae of *Argiocnemis rubescens rubeola* larva: (A, C) row of spiniform setae on anterior margin, (A) dorsal side, (C) ventral side; (B) median lamella; (D) lateral lamella. Scale (A, C) = 0.5 mm, (B, D) 1 mm.

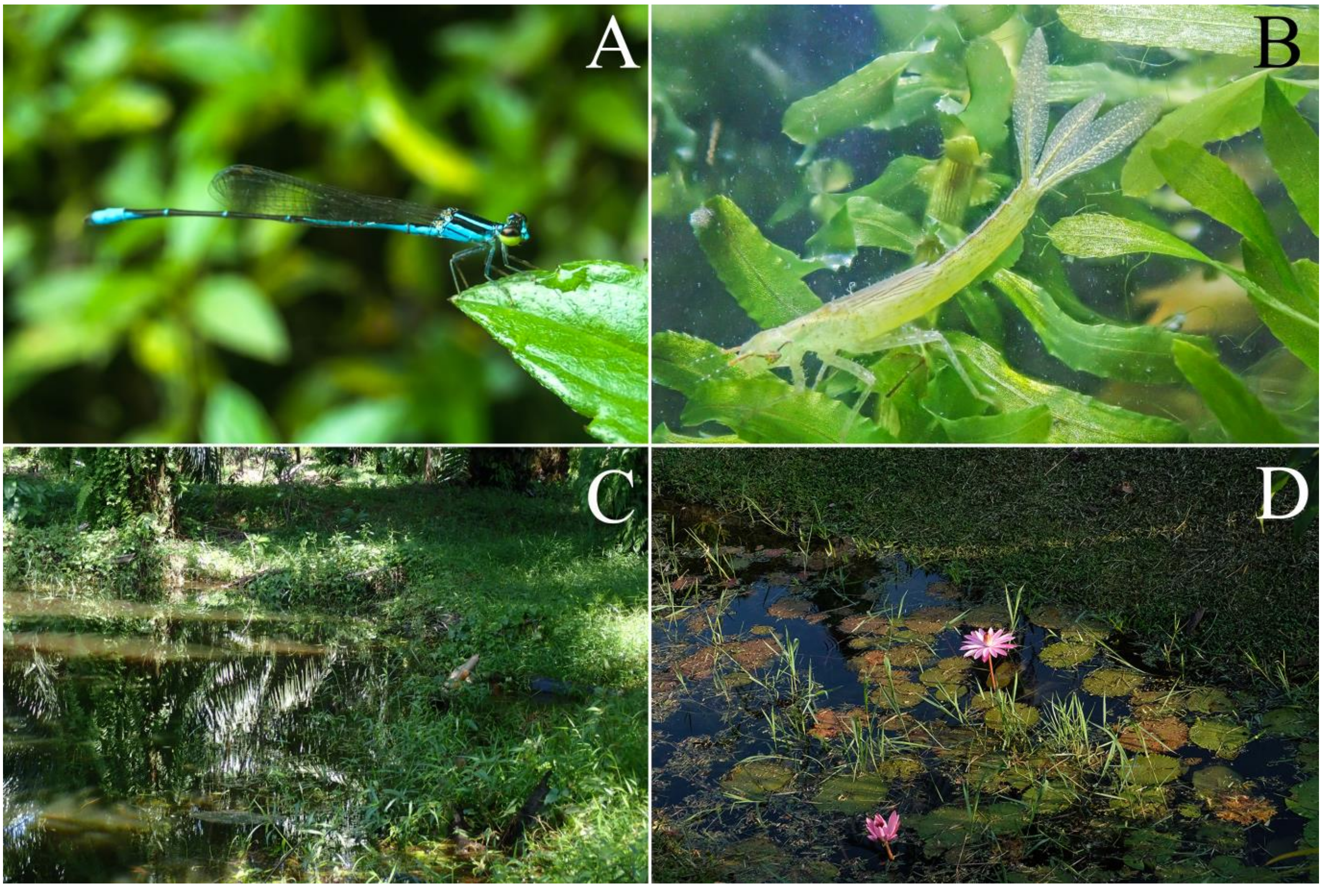

**FIGURE 8.** Adult, larva, and habitat of *Argiocnemis rubescens rubeola*: (A) adult in nature; (B) larva in aquarium; (C) pond in forest; (D) pond in Hala-Bala wildlife sanctuary.

***Biological notes.***— The adults of *Argiocnemis rubescens rubeola* can be found in lentic waters with dense vegetation (Figs. 8A, B). Their larvae usually inhabit the water adjacent to adults and both can be found in forest and agricultural ponds (Fig. 8C, D).

*Diagnosis*. The larvae of *Argiocnemis rubescens rubeola* in Thailand present a combination of characters typically found in the subfamily Agriocnemidinae (Ishida, 1996; Bae, 2011; Saetung and Boonsoong, 2019). However, the *A. r. rubeola* were different from the larval description of *A. r. rubescens* (in brackets) such as rounded postocular lobe [angulated], three premental setae [three or four], and four palpal setae [five] (Theischinger and Hawking, 2006).

## DISCUSSION

The four subspecies of *Argiocnemis rubescens* proposed by Lieftinck (1954) are *A. r. intermedia*, *A. r. lunulata*, *A. r. rubeola*, and *A. r. rubescens*. From the molecular results, *A. r. rubescens* and *A. r. rubeola* have an interspecific genetic distance of *COI* greater than 13% (sufficient to be individual species) (Ning et al., 2016; Tallei et al., 2017; Koroiva et al., 2017; Wu et al., 2019; Saetung & Boonsoong, 2019). Hence, research should focus on intensive fieldwork to acquire the necessary specimens and encompass diverse regions to ensure accurate determinations on taxonomic status of the subspecies of *Argiocnemis rubescens*, rather than relying on assumptions.

The *COI* tree depicting the prior relationships within the subfamily Agriocnemidinae indicated that the genus *Agriocnemis* formed a paraphyletic clade. Notably, *Argiocnemis* appears as a sister clade to *Agriocnemis* (*minima*-group). The Asian and Afrotropical species are grouped together as a distinct clade, except for *Agriocnemis forcipata*. The lineage of *Mortonagrion* mostly shows a polytomy. The taxonomic position is generally well-supported, but further investigation is required for a more thorough understanding of the *Agriocnemis* (minima-group). While the taxonomic hypothesis offers a swift overview, additional studies are required to clarify the relationship of these three genera.

Dow (2011) and Saetung and Boonsoong (2019) studied the relationships within the subfamily Agriocnemidinae, with a focus on genital ligula characteristics. Despite the similarity of the genital

**Key to the larvae of Asian genera of the subfamily Agriocnemidinae** (based on Ishida (1996); Bae (2011); Saetung and Boonsoong (2019); Bun (2024); Ng (2024))

**1** Labium with 3–5 pair premental setae (If 3 pair premental setae, with another one short seta) and 4–6 palpal setae; presence of band on caudal lamella ………………..……………………………….……. **2**

**1'** Labium with 3 pair premental setae and 4 palpal setae; lanceolate shape and absence of band on caudal lamella ……………………..……………………………………………………….…..… ***Argiocnemis***

**2** Llabium with 3–4 pairs premental setae (If 3 pair premental setae, with another one short seta) and 4–5 palpal setae, lanceolate or ovate shape of caudal lamella ………………………………….…. ***Agriocnemis***

**2'** Labium with 4–5 pairs premental setae (If 4 pair premental setae, with another one short seta) and 6 palpal setae, subulate shape of caudal lamella ……………………...……………………..…….. ***Mortonagrion***

ligula in *Argiocnemis* to that of *Agriocnemis* (minima-group), there are distinctions. Specifically, *Argiocnemis* exhibits a single row of teeth on the distal part of genital ligula segment 2, while *Agriocnemis* (minima-group) displays two rows of teeth (Saetung & Boonsoong, 2019). Additionally, the genital ligula of *Mortonagrion* exhibits variable shapes, as noted by Dow (2011). Larval characteristics serve as valuable indicators for understanding taxonomic relationships. The *Argiocnemis* larva differs significantly from *Agriocnemis* and *Mortonagrion* in terms of the shape of the postocular lobe (rounded shape: *Argiocnemis* and *Agriocnemis* [femina-group], angulated shape: *Mortonagrion* and *Agriocnemis* [minima-group]), shape of caudal lamella (lanceolate shape: *Argiocnemis* and *Agriocnemis*, subulate shape: *Mortonagrion*) and band on caudal lamella (absent: *Argiocnemis*, present: *Agriocnemis* and *Mortonagrion*) (Ishida, 1996; Bae, 2011; Saetung and Boonsoong, 2019; Bun, 2024; Ng, 2024).

The information derived from larval characteristics is consistent with both *COI* data and adult morphology, providing a comprehensive perspective. However, it is important to note that the current study's focus on the *COI* gene in mitochondrial DNA alone is not sufficient to draw lineage relationships. Further analyses, encompassing larval characteristics, nuclear genes, and additional mitochondrial genes are imperative for a comprehensive exploration of lineage relationships within the subfamily Agriocnemidinae.

## ACKNOWLEDGMENTS

The project was partially supported by the Basic Research Fund (BRF 6/2565) from the Faculty of Science, Kasetsart University, and the International Dragonfly Fund. This project was also joined under a Cooperative research and development agreement for material transfer between the Faculty of Science, Kasetsart University, and the National Institute of Advanced Industrial Science and Technology. We would like to thank Dr Akihiko Sasamoto, Dr Michal Sartori, Mr Noppadon Makbun, and Dr Rory A. Dow for their valuable suggestions and for providing the necessary literature for the present study. We would also like to thank the Department of Zoology, Faculty of Science, Kasetsart University, for the facilities provided, and we are also indebted to the Department of National Parks, Wildlife and Plant Conservation, Thailand, for permitting us to work and collect specimens.

## LITERATURE CITED

Asahina, S. 1993. A list of the Odonata from Thailand (Parts I–XXI). Bosco Offset, Bangkok, 460 pp.

Bae, Y.J. 2011. Insect Fauna of Korea Volume 4, Number 1 Arthropoda: Insecta: Odonata Zygoptera Damselflies. The National Institute of Biological Resources, Incheon, 66 pp.

Bun, T.H. 2024. Biodiversity of Singapore, Lee Kong Chian Natural History Museum (LKCNHM), Singapore, Available from: https://singapore.biodiversity.online/species/A-Arth-Hexa-Odonata-000048, (19/01/2024).

Clausnitzer, V. and Martens, A. 2004. Critical species of Odonata in the Comoros, Seychelles, Mascarenes and other small western Indian Ocean islands. International Journal of Odonatology, 7: 207–218.

Dijkstra,K.–D.B., Kipping, J. and Meziere, N. 2015. Sixty new dragonfly and damselfly species from Africa (Odonata). Odonatologica, 44(4): 447–678.

Dijkstra, K–D.B., Kalkman, V.J., Dow R.A., Stoks, F.R. and Van Tol, J. 2014. Redefining the damselfly families: a comprehensive molecular phylogeny of Zygoptera (Odonata). Systematic Entomology, 39(1): 68–96.

Dow, R.A. 2011. *Mortonagrion indraneil* spec. nov. from Borneo, and a redescription of *M. arthuri* Fraser (Odonata: Zygoptera: Coenagrionidae). Zootaxa, 3093(1): 35–46.

Edler, D., Klein, J., Antonelli, A. and Silvestro, D. 2020. raxmlGUI 2.0: A graphical interface and toolkit for phylogenetic analyses using RAxML. *Methods in Ecology and Evolution*.

Folmer, O., Black, M., Hoeh, W., Lutz, R. and Vrijenhoek, R. 1994. DNA primers for amplification of mitochondrial cytochrome oxidase subunit I from diverse metazoan invertebrates. Molecular Marine Biology and Biotechnology, 3: 294–299.

Fraser, F.C. 1934. The fauna of British India, including Ceylon and Burma. Odonata. Vol. II. Taylor and Francis, London, 398 pp.

Hall, T.A. 1999. BioEdit: A user-friendly biological sequence alignment editor and analysis program for Windows 95/98/NT. Nucleic Acids Symposium Series, 41: 95–98.

Huelsenbeck, J.P. and Ronquist, F. (2001) MRBAYES: Bayesian inference of phylogenetic trees. Bioinformatics, 17(8): 754–755.

Ishida, K. 1996. Monograph of Odonata larvae in Japan. Hokkaido University Press, Sapporo, 446 pp.

Kalkman, V.J. and Orr, A.G. 2013. Field Guide to the damselflies of New Guinea. Brachytron, supplement 16: 3–120.

Koroiva, R., Pepinelli, M., Rodrigues, M.E., Roque, F.O., Lorenz-Lemke, A.P. and Kvist, S. 2017. DNA barcoding of odonates from the Upper Plata basin: database creation and genetic diversity estimation. Plos One, 12: e0182283.

Kumar, S., Stecher, G., Li, M., Knyaz, C. & Tamura, K. 2018. MEGA X: Molecular Evolutionary Genetics Analysis across computing platforms. *Molecular Biology and Evolution*. 35, 1547–1549.

Lieftinck, M.A. 1954. Handlist of Malaysian Odonata. A catalogue of the dragonflies of the Malay Pensinsula, Sumatra, Java and Borneo, including the adjacent small islands. Treubia, 22: xxiv–202.

Morse, J.C., Yang, L. and Tian, L. 1994. Aquatic Insects of China Useful for Monitoring Water Quality. Hohai University Press, Nanjing, 570 pp.

Needham, J.G. 1930. A Manual of the Dragonflies of China. The Fan Memorial Institute of Biology, Peiping, 344 pp.

Ng, M. 2024. Biodiversity of Singapore, Lee Kong Chian Natural History Museum (LKCNHM), Singapore, Available from: https://singapore.biodiversity.online/species/A-Arth-Hexa-Odonata-000014, (19/01/2024).

Ning, X., Kompier, T., Yu, X. and Bu, W. 2016. *Paracercion ambiguum* sp. nov. from Lang Son, Vietnam (Zygoptera: Coenagrionidae). *Zootaxa*, 4144 (2): 263–275.

Paulson, D., Schorr, M., Abbott, J., Bota-Sierra, C., Deliry, C., Dijkstra, K.–D.B. and Lozano, F. 2023. World Odonata List. OdonataCentral, University of Alabama. Available from: https://www.odonatacentral.org/app/#/wol/. (01/Mar./2023).

Puillandre, N., Brouillet, S., Achaz, G. 2020. ASAP: Assemble species by automatic partitioning. *Molecular Ecology Resources*, 21(2): 609–620.

Rambaut, A. 2012. FigTree. Version 1.4. Available from: http://tree.bio.ed.ac.uk/software/figtree (accessed 23 August 2023)

Saetung, T. and Boonsoong, B. 2019. A review of genus *Agriocnemis* larva (Odonata: Coenagrionidae) from Thailand including a description of the final stadium larva of *Agriocnemis minima* Selys, 1877 with supporting molecular (COI) data. Zootaxa, 4711(3): 579–599.

Steinmann, H. 1997. World Catalogue of Odonata I: Zygoptera, Parts 110-111 of Das Tierreich. The Animal Kingdom Series Issue 110 of World Catalogue of Odonata, Henrik Steinmann. Walter de Gruyter &co., Berlin, 521 pp.

Tallei, T.E., Koneri, R. and Kolondam, B.J. 2017. Sequence Analysis of the Cytochrome C Oxidase Subunit I Gene of *Pseudagrion pilidorsum* (Odonata: Coenagrionidae). Makara Journal of Science, 21(1): 43–52.

Theischinger, G. and Hawking, J. H. 2006. The Complete Field Guide to Dragonflies of Australia. CSIRO Publishing, Collingwood, 377 pp.

Theischinger, G. and Endersby, I. 2009. Identification Guide to the Australian Odonata. Department of Environment, Climate Change and Water NSW, Sydney, 290 pp.

Tillyard, R.J. 1917. On the morphology of the caudal gills of the larvae of zygopterid dragonflies. The Proceedings of the Linnean Society of New South Wales, 42: 32–118.

Thipaksorn, A., Apiwathnasorn, C., Ruangsittichai, J. 2012. Modified molecular techniques for detection rice Odonate insects in Thailand. Munis Entomology and Zoology, 7(2): 852–856.

Thipaksorn, A., Ruangsittichai, J. 2010. Diversity of rice odonate insects in Lopburi province, Thailand. New Entomologist, 59(3, 4): 37-42.

Watson, M.C. 1956. The utilization of mandibular armature in taxonomic studies of anisopterous nymphs. Transactions of the American Entomological Society, 81: 155–202.

Wu, X., Liu, Z., Chen, Y., and Wang, B. 2019. Description of larva of *Euphaea superba* Kimmins, 1936 (Odonata: Zygoptera: Euphaeidae) from China. Zootaxa, 4545(4): 585–592.

Zhang, J., Kapli, P., Pavlidis, P. and Stamatakis, A. 2013. A general species delimitation method with applications to phylogenetic placements. *Bioinformatics*, 29: 2869–2876.